Collisional-Radiative Equilibrium (CRE) Model for the CONRAD Radiation-Hydrodynamics Code

J.J. MacFarlane

December 1993

UWFDM-937

FUSION TECHNOLOGY INSTITUTE

UNIVERSITY OF WISCONSIN

MADISON WISCONSIN

Collisional-Radiative Equilibrium (CRE) Model for the CONRAD Radiation-Hydrodynamics Code

J. J. MacFarlane

Fusion Technology Institute
Department of Nuclear Engineering and Engineering Physics
University of Wisconsin-Madison
Madison, WI 53706

December 1993

UWFDM-937

Contents

1. Introduction

Radiative transfer effects often play a crucial role in the energetics of high temperature laboratory plasmas [1-11]. For example, in targets irradiated by intense laser or ion beams, radiative energy losses from the target plasma can significantly affect its hydrodynamic evolution [5,6]. A good understanding of the dynamics and energetics of such high temperature plasmas can often be gained from radiation-hydrodynamics simulations. Because of its importance, it is crucial that radiative transfer be modeled accurately.

As noted in earlier work [8,10], multigroup radiation diffusion models, which are commonly used in radiation-hydrodynamics codes, can sometimes be very inaccurate for simulating the radiative properties of laboratory plasmas. This is especially true for plasmas which are optically thick to line radiation but optically thin to the continuum. This occurs for several reasons. First, resonant self-absorption — that is, the trapping of line radiation in their optically thick cores — can significantly inhibit the flow of radiation through the plasma. This cannot be accurately treated in "multigroup" models unless the photon energy grid is chosen such that individual lines are resolved. Second, high temperature laboratory plasmas are often not in local thermodynamic equilibrium (LTE). In many cases, the atomic level populations — and therefore the opacities — are a function of not only the local temperature and density, but also the radiation field. Because of this, models utilizing table look-up opacities which depend only on the temperature and densities can be inaccurate. Third, radiation diffusion models are based on the assumption that the photon mean free paths are small compared to the plasma dimensions. This assumption is also not valid for many types of laboratory plasmas.

In this report, we describe the features of a radiation transport algorithm we have developed to investigate the radiative properties of high energy density plasmas. This is a non-LTE radiative transfer model, or collisional-radiative equilibrium (CRE) model, which can be used to calculate emission and absorption spectra, as well as radiative energy transport. The major features of the physics models have been described elsewhere [12-16], and only an overview of them will be presented here. This report is intended to be a "users' guide." Thus, the focus here will be on the structure of the algorithms, how they interface with CONRAD [9], and how to use them. A users' guide for the atomic physics package which sets up atomic data files for the radiative transfer model is presented elsewhere [17].

Given a temperature and density distribution for a plasma, the CRE model computes atomic level populations and the radiative flux through the plasma. The models are 1-D, and can be applied to plasmas in planar, cylindrical, and spherical geometries. Opacity effects are considered in computing both the atomic level populations (via photoexcitation and photoionization) and the radiation flux.

Sections 2 through 4 of this report provide brief descriptions of the statistical equilibrium, radiative transfer, and atomic physics models. A description of the interfacing between the CRE/radiative transfer modules and CONRAD is provided in Section 5. Input and output files are described in Section 6, while the namelist input used to set up a calculation is detailed in Section 7. The subroutines and common block descriptions are provided in Sections 8 and 9, respectively.

2. Statistical Equilibrium Model

Atomic level populations are calculated by solving multilevel, steady-state atomic rate equations self-consistently with the radiation field. For multilevel systems, the rate equation for atomic level i can be written as:

$$\frac{dn_i}{dt} = -n_i \sum_{j \neq i}^{N_L} W_{ij} + \sum_{j \neq i}^{N_L} n_j \, W_{ji} = 0 \,, \tag{2.1}$$

where W_{ij} and W_{ji} represent the depopulating and populating rates between levels i and j, n_i is the number density of level i, and N_L is the total number of levels in the system. For upward transitions ($i < j$),

$$\begin{aligned} W_{ij} &= B_{ij} \, \bar{J}_{ij} + n_e \, C_{ij} + \\ &+ \beta_{ij} + n_e \, \gamma_{ij} \,, \end{aligned} \tag{2.2}$$

while for downward transitions,

$$\begin{aligned} W_{ji} &= A_{ji} + B_{ji} \, \bar{J}_{ji} + n_e \, D_{ji} + \\ &+ n_e \, (\alpha_{ji}^{RR} + \alpha_{ji}^{DR}) + n_e^2 \, \delta_{ji} \,, \end{aligned} \tag{2.3}$$

where n_e is the electron density and $\bar{J}_{ij}$ ($\equiv \int \phi_{ij}(\nu) \, J_\nu \, d_\nu$) is the frequency-averaged mean intensity of the radiation field for a bound-bound transition. The rate coefficients in the above equations are:

$$\begin{aligned} A_{ij} &= \text{spontaneous emission} \\ B_{ij} &= \text{stimulated absorption } (i < j) \text{ or emission } (i > j) \\ C_{ij} &= \text{collisional excitation} \\ D_{ij} &= \text{collisional deexcitation} \\ \alpha_{ij}^{RR} &= \text{radiative recombination} \\ \alpha_{ij}^{DR} &= \text{dielectronic recombination} \\ \beta_{ij} &= \text{photoionization plus stimulated recombination} \\ \gamma_{ij} &= \text{collisional ionization} \\ \delta_{ij} &= \text{collisional recombination.} \end{aligned}$$

Atomic cross sections for the above terms are described briefly in Section 4. In this detailed configuration accounting model each atomic level of a given gas species can in

principle be coupled to any other level in that gas. The degree of coupling between levels depends on how the atomic data files are generated by ATBASE [17].

The statistical equilibrium equations (Eq. (2.1)) depend on the atomic level populations in a nonlinear fashion (through the radiation intensity and electron density). Because of this, an iterative procedure is used to obtain atomic level populations which are self-consistent with the radiation field. At present, the coupled set of steady-state rate equations is solved using the LAPACK linear algebra package [18]. Besides inverting the statistical equilibrium equation matrix to obtain the level populations, LAPACK also contains algorithms for improving the condition of the matrix via scaling, as well as iterative refinement. The overall procedure for computing the level populations is as follows:

1. Make an initial guess for population distributions (e.g., LTE, optically thin, or populations from previous hydrodynamics time step)
2. Compute radiative rate coefficients
3. Compute coefficients for statistical equilibrium matrix ($N_L \times N_L$)
4. Solve matrix for level populations
5. If new populations are consistent with previous iteration, calculation is complete; otherwise go back to step 2.

Steps 2 through 4 are performed one spatial zone at a time. This is possible because we employ an accelerated lambda iteration procedure (ALI) which utilizes the diagonal of the Λ-operator [19,20; see also Section 3].

To improve the rate of convergence for this iterative procedure we utilize an acceleration technique based on the work of Ng [21; see also 22, 20]. The Ng acceleration method is applied every several (typically 2 to 6) iterations to obtain updated solutions to the solution vector $\mathbf{x}$. In our case, the solution vector is the level population of a spatial zone. The "accelerated" solution is calculated from solutions obtained during the previous several iterations — that is, the evolution, or history, of the convergence becomes important. The accelerated solution vector after the n'th iteration can be written as:

$$\mathbf{x}^n = \left(1 - \sum_{m=1}^{M} \alpha_m\right) \mathbf{x}^{n-1} + \sum_{m=1}^{M} \alpha_m \mathbf{x}^{n-m-1}, \tag{2.4}$$

where $\mathbf{x}^{m-n}$ is the solution vector of the (n−m)'th iteration. The acceleration coefficients, α, are determined from the solution of

$$\mathbf{A}\alpha = \mathbf{b}, \tag{2.5}$$

where the elements of $\mathbf{A}$ and $\mathbf{b}$ are given by:

$$\begin{aligned} A_{ij} &= \sum_{d=1}^{D} (\Delta x_d^n - \Delta x_d^{n-i})(\Delta x_d^n - \Delta x_d^{n-j}), \\ b_i &= \sum_{d=1}^{D} \Delta x_d^n (\Delta x_d^n - \Delta x_d^{n-i}), \end{aligned} \tag{2.6}$$

and

$$\Delta x_d^k \equiv x_d^k - x_d^{k-i}.$$

The quantity x_d^k refers to the d'th element of $\mathbf{x}$ on iteration cycle k. The order of the acceleration method, M, represents the number of previous cycles used to compute the accelerated solution for $\mathbf{x}$.

In our radiative transfer code M can be chosen to have a value from 2 to 4. It is found that using $M = 2$ provides very good acceleration to the converged solution. This method has proven to be particularly valuable in improving the computational efficiency of our radiative transfer simulations.

3. Radiative Transfer Model

The CRE algorithms utilize an angle- and frequency-averaged escape probability model. The advantage of the escape probability model is that it is fast; i.e., it is a computationally efficient method for computing resonant self-absorption effects on both the non-LTE atomic level populations and the radiation flux. In this model, the stimulated absorption and emission rates in Eqs. (2.2) and (2.3) can be written in terms of zone-to-zone coupling coefficients:

$$n_j^a\, B_{ji}\, \bar{J}_{ij} - n_i^a\, B_{ij}\, \bar{J}_{ij} = \begin{cases} -A_{ji}\, \sum_{e=1}^{N_D}\, n_j^e\, Q_{ji}^{ea} & (i < j) \\ \\ A_{ij}\, \sum_{e=1}^{N_D}\, n_i^e\, Q_{ij}^{ea} & (i > j) \end{cases}$$

where Q^{ea} is defined as the probability a photon emitted in zone e is absorbed in zone a, n_i is the population density of level i, the superscripts e and a denote the emitting and absorbing zones, respectively, and N_D is the number of spatial zones. Our model utilizes a computationally efficient method for computing angle- and frequency-averaged escape probability coupling coefficients in planar, cylindrical, and spherical geometries for Doppler, Lorentz, and Voigt line profiles. (This method is based largely on the work of J. Apruzese et al. [23-25].)

Consider first the 1-D planar geometry shown in Fig. 3.1. The distance traversed as a photon travels from point 1 to point 2 is z_{12}/μ, where $\mu \equiv \cos\theta$ and θ is the angle between the direction of propagation and the normal to the slab surface. In this geometry, the angle- and frequency-averaged escape probability, $\overline{P_e}$, can be computed directly:

$$\overline{P_e}(\tau_c) = \int_0^1\, P_e(\tau_c/\mu)\, d\mu\,, \tag{3.1}$$

where P_e is the frequency-averaged escape probability (described below). The probability a photon emitted in zone e traverses a depth τ_B between zones e and a, and is then absorbed in zone a is

$$Q^{ea} = \frac{1}{2\tau_e}\, \int_0^{\tau_e}\, [\bar{P}_e(\tau_B + \tau) - \bar{P}_e(\tau_B + \tau_a + \tau)]\, d\tau\,. \tag{3.2}$$

Note that τ_e, τ_B, and τ_a are the optical depths in the direction normal to the slab surface. The first term within the integral represents the probability a photon will get to the nearer surface of zone a without being absorbed, while the second term represents the probability the photon is absorbed before exiting the surface farther from zone e. The coupling coefficients are efficiently computed using analytic expressions.

Evaluation of the coupling coefficients in cylindrical and spherical geometries is more difficult because Eq. (3.1) is not valid and angle-averaged escape probabilities

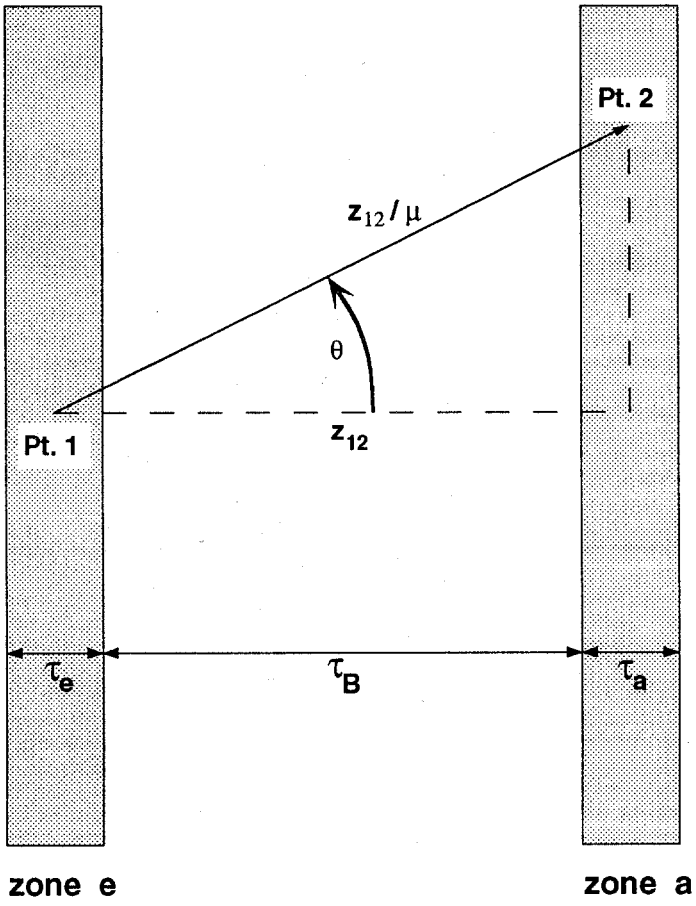

Figure 3.1. Schematic illustration of photon transport in planar geometry.

cannot be computed directly. For these geometries, it was found [24] that introducing a "mean diffusivity angle," $\bar{\theta} \equiv \cos^{-1}\bar{\mu}$, for which

$$P_e\left(\frac{\tau}{\bar{\mu}}\right) \cong \int_0^1 P_e\left(\frac{\tau}{\mu}\right) d\mu\,, \tag{3.3}$$

leads to solutions that compare reasonably well with exact solutions. The meaning of the mean diffusivity angle is clarified in Fig. 3.2. The quantities τ_e, τ_a, and τ_B again represent the line center optical depths of the emitting and absorbing zones and the depth between them, respectively. In this case, however, the optical depths are computed along the ray defined by $\bar{\theta}$ and the midpoint of the emitting zone.

It can also be seen from Fig. 3.2 that additional geometrical complications arise when the absorbing zone is inside the emitting zone. To overcome this, while at the same time maintaining computational efficiency, we take advantage of the reciprocity relation:

$$N^i Q^{ij} = N^j Q^{ji}\,, \tag{3.4}$$

where N^i and N^j are the total number of absorbing atoms in zones i and j, respectively. (A proof of this relation is given in Ref. [24]). Thus, in cylindrical and spherical geometries the coupling coefficients are given by:

$$Q^{ea} = \frac{1}{\tau_e}\int_0^{\tau_e} \left[P_e(\tau_B+\tau) - P_e(\tau_B+\tau_a+\tau)\right] d\tau\,, \tag{3.5}$$

where P_e is the non-angle-averaged escape probability. The Q^{ea} are calculated using Eq. (3.5) only for the cases when the absorbing zone is at a larger radius than the emitting zone. Otherwise, the reciprocity relation (Eq. (3.4)) is used. It has been shown [24] that using $\bar{\mu} = 0.51$ leads to solutions for 2-level atoms that are accurate to within 25% for a wide range of total optical depths.

The frequency-averaged probability a photon will traverse a distance equivalent to a line center optical depth τ_c is:

$$P_e(\tau_c) = \int_0^\infty \phi(\nu)\, e^{-\tau_\nu} d\nu\,, \tag{3.6}$$

where $\phi(\nu)$ is the normalized line profile ($\int \phi(\nu)\, d\nu = 1$), and

$$\tau_\nu = \tau_c \phi(\nu)/\phi(\nu_0)\,.$$

The quantity ν_0 represents the frequency at line center.

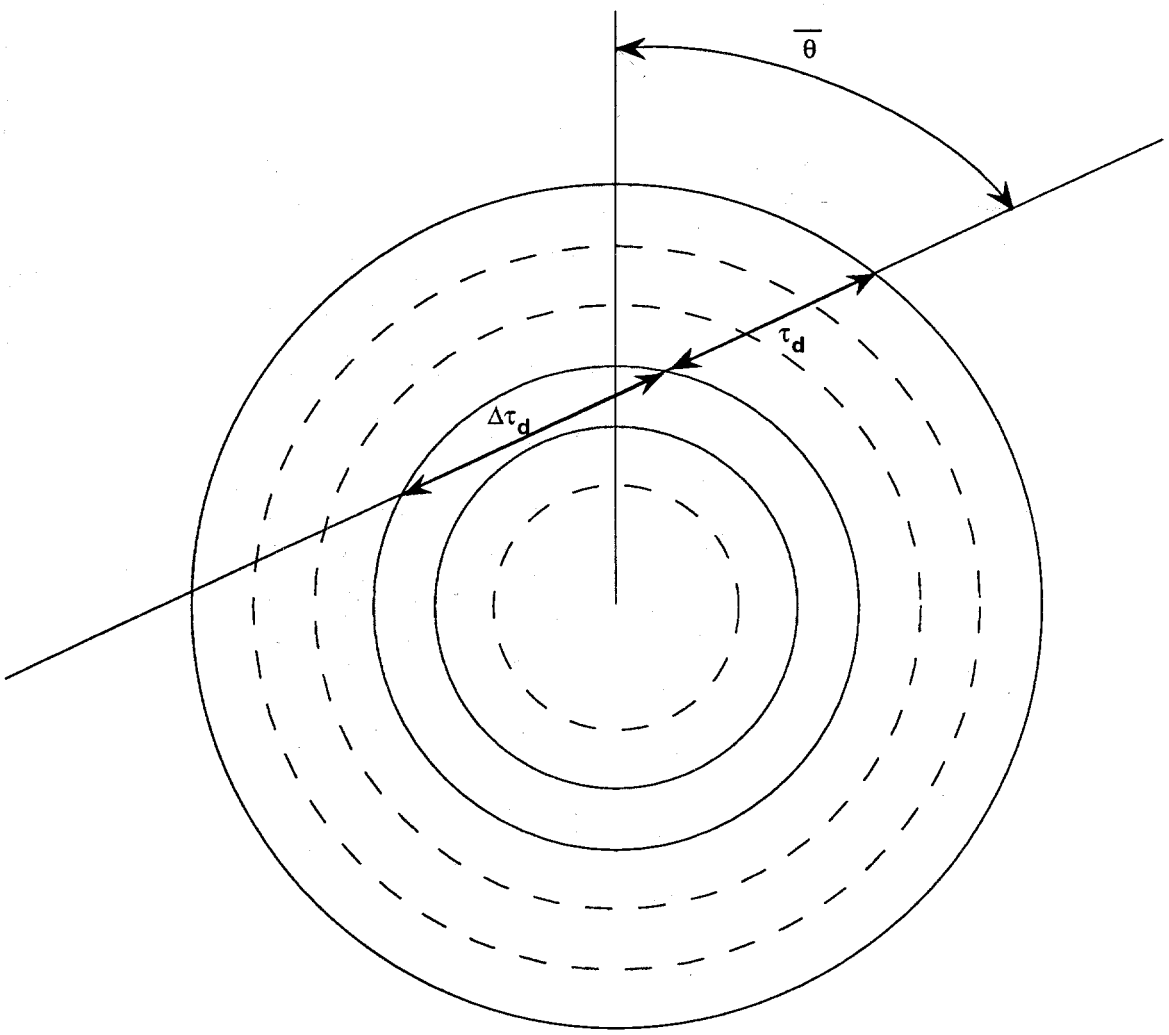

Figure 3.2. Schematic illustration of photon transport in cylindrical and spherical geometries.

The profiles considered for bound-bound transitions are:

$$\begin{aligned}
&\text{Doppler}: \quad \phi(\nu) = (\pi^{1/2}\Delta\nu_D)^{-1}\, e^{-x_D^2}\,, && x_D = \tfrac{\nu-\nu_0}{\Delta\nu_D} \\
&\text{Lorentz}: \quad \phi(\nu) = \tfrac{4}{\Gamma}\tfrac{1}{1+x_L^2}\,, && x_L = \tfrac{4\pi}{\Gamma}\,(\nu-\nu_0) \\
&\text{Voigt}: \quad \phi(\nu) = (\pi^{1/2}\Delta\nu_D)^{-1}\, H(a,x_D)\,, && a = \tfrac{\Gamma}{4\pi\Delta\nu_D}\,.
\end{aligned} \tag{3.7}$$

The parameter Γ can be interpreted as the reciprocal of the mean lifetimes of the upper and lower states, $\Delta\nu_D$ is the Doppler width of the line, and

$$H(a,x_D) = \frac{a}{\pi}\int_{-\infty}^{\infty} \frac{e^{-y^2}}{(x_D-y)^2+a^2} \tag{3.8}$$

is the Voigt function [26].

In evaluating the escape probability integrals we use an approach similar to that of Apruzese et al. [23-25]. Simple analytic fits to accurate numerical solutions to the frequency-averaged escape probabilities were obtained for each profile. For bound-bound transitions, complete frequency redistribution is assumed; i.e., the emission and absorption profiles are identical.

For Doppler profiles we use:

$$P_e(\tau_c) = \begin{cases} 2.329\,[\tan^{-1}(0.675\tau_c+0.757)-\tan^{-1}(0.757)]\,, & \tau_c \le 5.18 \\ \\ 0.209+1.094\,[\ln\tau_c]^{1/2}\,, & \tau_c > 5.18\,, \end{cases} \tag{3.9}$$

while for Lorentz profiles we use:

$$P_e(\tau_c) = \begin{cases} 1.707\ln(1+0.586\,\tau_c)\,, & \tau_c \le 5.18 \\ \\ -0.187+1.128\,\tau_c^{1/2}\,, & \tau_c > 5.18\,. \end{cases} \tag{3.10}$$

For Voigt profiles, the escape probability integrals were fitted to two different regimes of the Voigt broadening parameter a. For $a < 0.49$,

$$P_e(\tau) = \begin{cases} (1+1.5\tau)^{-1} & (\tau \le 1), \\ \\ 0.4\tau^{-1} & (1 < \tau \le \tau_c), \\ \\ 0.4(\tau_c\tau)^{-1/2} & (\tau > \tau_c), \end{cases} \tag{3.11}$$

where

$$\tau_c \equiv \frac{0.83}{a(1+a^{1/2})}.$$

For $a \geq 0.49$,

$$P_e(\tau) = \begin{cases} (1+\tau)^{-1} & (\tau \leq 1), \\ \\ 0.5\ \tau^{-1/2} & (\tau > 1). \end{cases} \tag{3.12}$$

The fits for Voigt profiles are typically accurate to about 20%, although errors of up to 40% can occur. Note, however, that in our model the frequency-averaged escape probability integrals are used only to compute the level populations self-consistently with the radiation field. The frequency-dependent spectral calculations do not directly use frequency-averaged escape probabilities.

We now discuss the transport of bound-free radiation in the context of the escape probability model. The frequency-averaged escape probability is obtained by averaging the attenuation factor, $e^{-\tau_\nu}$, over the emission profile ϕ_E:

$$P_e(\tau_0, \alpha_0) = \int_{\nu_1}^{\infty} \phi_E(\nu, \alpha_0) \exp(-\tau_\nu) d\nu, \tag{3.13}$$

where

$$\phi_E(\nu, \alpha_0) = \frac{\exp(-h\nu/kT_e)}{\nu E_1(\alpha_0)}$$

and

$$\alpha_0 \equiv h\nu_1/kT_e.$$

The optical depth and frequency at the photoionization edge are τ_0 and ν_1, respectively, τ_ν is the optical depth at frequency ν, T_e is the electron temperature, and $E_1(x)$ represents the exponential integral of order 1. The quantities h and k as usual refer to the Planck constant and Boltzmann constant, respectively.

As in the case of line transport, frequency-averaged escape probabilities have been fitted to simple analytic functions to allow for computationally efficient solutions. The curve fits are given by:

$$P_e(\tau_0, \alpha_0) = \begin{cases} e^{-\gamma_1 t} & , \quad t \leq 1.0 \\ \\ t^{-1/3} \exp[-\gamma_1 - \gamma_2 (t^{1/3} - 1)] & , \quad t > 1.0 \end{cases} \tag{3.14}$$

where

$$\begin{aligned} \gamma_1(\alpha_0) &= 2.01\alpha_0 - 1.23\alpha_0^{3/2} + 0.210\alpha_0^2, \\ \gamma_2(\alpha_0) &= 1.01\alpha_0 + 0.0691\alpha_0^{3/2} - 0.0462\alpha_0^2, \end{aligned}$$

and $t \equiv \tau_0/3$. The fits are accurate to about 15% over a wide range of parameter space: $0.3 < \alpha_0 < 10$ and values of τ_0 such that $P_e(\tau_0, \alpha_0) \geq 10^{-5}$.

The photoionization rate in zone a is obtained by summing the recombinations over all emitting zones e. Thus, the photoionization rate (corrected for stimulated recombinations) from lower level ℓ to upper level u can be written as:

$$\begin{aligned} \beta_{\ell u} &= 4\pi \int_{\nu_o}^{\infty} \frac{\alpha_\nu^{bf}}{h\nu} J_\nu^a \left(1 - \left(\frac{n_u^a}{n_\ell^a}\right) \left(\frac{n_\ell^a}{n_u^a}\right)^* e^{-h\nu/kT_e}\right) d\nu \\ &= \sum_{e=1}^{N_D} N_u^e \, n_e^e \, \alpha_{rr}^e \, Q^{ea}, \end{aligned} \tag{3.15}$$

where α_ν^{bf} is the photoionization cross section, J_ν is the radiation mean intensity, $(n_\ell/n_u)^*$ refers to the LTE population ratio [26], α_{rr}^e is the radiative recombination rate coefficient for zone e, n_e^e is the electron density in zone e, and N_D is the total number of spatial zones in the plasma.

4. Atomic Physics Models

Atomic structure calculations for energy levels are performed using a configuration interaction (CI) model using Hartree-Fock wavefunctions [17,27]. An L-S coupling scheme is used to define the angular momentum coupling of electrons. Rate coefficients for collisional and radiative transitions are calculated as follows. Collisional excitation and ionization rates are computed using a combination of semiclassical impact parameter, Born-Oppenheimer, and distorted wave models [28-30]. The corresponding inverse processes were specified from detailed balance arguments. Rate coefficients for dielectronic recombination are computed using a Burgess-Mertz model [31] in conjunction with Hartree-Fock energies and oscillator strengths. Photoionization cross sections and radiative recombination rates are obtained from Hartree-Fock calculations. Details of the atomic physics calculations are given elsewhere [17,27].

5. Interface Between CRE and Radiation-Hydrodynamics Models

5.1. Overview of CRE/Radiation-Hydrodynamics Coupling

At present, the CRE model is coupled to CONRAD as follows. Line radiation and continuum radiation are transported separately. The continuum radiation, which includes bound-free and free-free processes, is transported using the previously existing multigroup radiation diffusion model in CONRAD. This approach should provide a reasonable approximation because continuum opacities vary relatively smoothly with frequency (i.e., compared to bound-bound transitons). Continuum opacities for each photon energy group in this case are a function of the local density and temperature, but independent of the radiation field.

Line radiation is transported using the CRE escape probability model. Here, the rate at which energy is gained (absorbed) and lost (emitted) in each spatial zone is computed for each bound-bound transition. This transfer of energy is then included in the radiation-hydrodynamics plasma energy equation as a "source" term. The plasma energy equation for each spatial zone can be written as:

$$De/Dt = -D(u^2/2)/Dt + \rho^{-1}\nabla\cdot(pu) - J + A + S \tag{5.1}$$

where e is the plasma specific internal energy, u is the fluid velocity, p is the pressure, ρ is the density, A and J are the radiation absorption and emission terms, and S is a source term (which includes, for example, ion beam energy deposition). Thus, the internal energy at time t_{n+1} is given by:

$$e(t_{n+1}) = e(t_n) + (t_{n+1} - t_n)\, De/Dt\,. \tag{5.2}$$

The various contributions to De/Dt are evaluated using the plasma conditions at t_n. This form of time stepping is first order accurate in time. This approach has been applied successfully by others in a wide variety of studies [32].

Once $T(r), n_e(r)$, and the atomic level populations are known, the radiation emission and absorption rates are easily computed from the zone-to-zone coupling coefficients, Q^{ea}. The emission rate in zone d due to all bound-bound transitions can be written as:

$$J^d = \sum_{u>\ell} \Delta E_{u\ell}\, A_{u\ell}\, n_u^d \tag{5.3}$$

where $A_{u\ell}$ is the spontaneous emissison rate for the transition $u \rightarrow \ell$, $\Delta E_{u\ell}$ is the transition energy, and n_u^d is the number density of atoms in the upper state of the

transition in zone d. To determine the absorption rate for zone d, we add the contribution of photons emitted in each zone:

$$A^d = (\Delta V^d)^{-1} \sum_{u>\ell} \Delta E_{u\ell}\, A_{u\ell} \sum_e n_u^e\, \Delta V^e\, Q^{ed} \tag{5.4}$$

where ΔV^d is the volume of zone d.

The radiant energy flux escaping at the plasma boundary at each time step is computed by subtracting the absorption rate for all zones from the emission rate summed over zones:

$$F_{surface} = (Area)^{-1} \sum_{u>\ell} \Delta E_{u\ell}\, A_{u\ell} \sum_e n_u^e\, \Delta V^e\, (1 - \sum_a Q^{ea})\,. \tag{5.5}$$

5.2. Mechanics of CRE/Radiation-Hydrodynamics Interface

The interfacing between the CRE and radiation-hydrodynamics (R-H) models occurs at the following points (see also Fig. 8.1):

- initialization and input,
- R-H plasma energy algorithm, and
- R-H radiation-dependent algorithms.

A single variable (NLTEID in CONRAD) must be read in during input to the R-H simulation to invoke the CRE line transport calculation. If the CRE model is not invoked, the above interface points are bypassed, in which case all CRE input and output files are not utilized.

Four CRE routines are utilized during the R-H initialization procedure:

- BDATAC – a block data routine
- CLEARC – initializes several variables to zero
- INNLTE – reads input for CRE model
- INITC1 – performs some CRE initializations

The last three subroutines are called from the R-H initialization/input subroutine.

Four CRE subroutines are called from one of the R-H plasma energy subroutines for each hydrodynamic time step:

- LODCB1 – loads R-H variables into CRE common blocks
- NLPOPS – computes atomic level populations
- LINRAD – computes line radiation emission and absorption rates for each spatial zone
- LODCB2 – stores CRE results in R-H common blocks.

The CRE line transport algorithms are invoked during each time cycle of the R-H simulation prior to the solution of the plasma energy equation. The results are stored in the CRE common block /CREOUT/ (see also Section 9). The results are then read into R-H common block for use in the following algorithms:

- computation of plasma energy source term
- computation of flux across outer plasma boundary
- monitoring of energy conservation
- output.

The variable names used in the above algorithms are given in subroutine LODCB2.

6. Input/Output File Descriptions

The CRE algorithms utilize up to 3 input files, 6 output files, and 1 scratch file. The files are listed in Table 6.1, along with their default logical unit numbers (LUN), names (for UNIX systems), types, and a brief description of their contents. (Note that the LUNs and file names can be easily modified in the block data routine BDATAC.) For each plasma species, two input files are required containing atomic data computed by the ATBASE suite of atomic physics codes [17]. These files (LUNs 4 and 8) are required for all calculations in which the CRE radiative transfer model is invoked. LUN 4 contains data for atomic level energies, oscillator strengths, collisional rate coefficients, and dielectronic recombination rate coefficients. LUN 8 contains photoionization cross section data.

Most parameters utilized by the CRE algorithms are specified in the namelist input file (LUN 2). Details concerning variable names and definitions are given in Section 7. The CRE model is invoked in CONRAD using the variable NLTEID. LUN 6 contains the descriptive output, including results for atomic level populations, ionization distributions, line radiation power densities, and debug output.

Several other output files provide results that can be used to analyze a problem. LUNs 41 and 42 contain transition rate information, which can be used to determine the most important transitions which populate and depopulate the various atomic levels. LUN 3 is used to write warning messages, the purpose of which is used to warn the user of potential problems that may have occurred during the calculation without stopping the calculation. LUN59 sets up a namelist input file which can be read in by the standalone CRE code NLTERT [33]. This is often quite helpful for debugging purposes.

Table 6.1. Input/Output Files

Default Unit Number	Default Name (UNIX)	Type	Description
2	cre.inp	Input	Namelist input for CRE radiative transfer parameters
3	cre.warnings	Output	Warning messages which occur during run time
4	rt.atom.dat.NN	Input	Atomic structure data (energy levels, oscillator strengths, collisional rate coefficients)
6	cre.out*	Output	Standard output (level populations, ionization distributions, line radiation power densities)
8	pixsec.dat.NN	Input	Photoionization cross sections
12	cre.popul.dat	Output	Atomic level populations
41	rate1	Output	Transition rate tables
42	rate2	Output	Rate coefficient tables
55	rt.scratch	Scratch	Scratch file
59	rt.inp.debug	Output	Writes namelist input file for testing with standalone NLTERT code

*Output file name for file 6 will usually be the radiation-hydrodynamics output file.
NN = atomic number of target plasma

7. Namelist Input Variables

The user defines the parameters for the CRE model from the namelist input file. Through it, the user specifies parameters for the atomic and radiative transfer models. In addition, the user can specify the types of plot output desired, and request the printing of various debugging output. Table 7.1 lists each of the namelist variable names, along with their type, dimensions, units, default values, and a brief description of their use. Comments can be inserted in the CRE namelist input file to aid the user. Lines starting with 'c ' in the namelist input file are considered comments. Note that the 'c ' must be in the first column, and must be followed by a space.

The atomic model parameters specify the distribution of atomic species in the plasma. Homogeneous mixtures as well as multilayered target plasmas can be modelled. Examples of this are shown in Table 7.1. Input files for each atomic species are automatically read in based on the atomic numbers specified (ATOMNM).

The selection of atomic levels included in the calculation is done through the variable ISELCT. This is a two-dimensional array arranged as [atomic level index, gas species]. By default, no levels are selected (all elements are zero). The user selects levels from the atomic data file (LUN 4) for each plasma species by setting the corresponding ISELCT array element to 1. For example, if one wishes to include level 85 from gas species 1, one simply sets ISELCT(85,1)=1. It is often useful to set up the selection process ion by ion. Thus, if level 85 were the ground state of some ion, the lowest 20 energy levels of that ion could be selected by setting ISELCT(85,1)=20*1.

The variable ILINEP (listed under Radiative Transfer Parameters) is used to set the line profile type. For laboratory plasmas, a Voigt profile should generally be used. Natural, Doppler, and Stark broadening effects are automatically included in the calculation. ISWCRE(7) and ISWCRE(8) are used to specify whether photoexcitation and photoionization be considered in the statistical equilibrium equations.

By default, the calculation of atomic level populations is performed by solving multilevel statistical equilibrium equations which include both collisional and radiative terms. However, the user can specify that LTE populations be computed by setting ISW(6)=3. ISW(6) is also used to specify the initial guess at the populations. In addition, transition rates for each type of process can be adjusted (or set to zero) by redefining CONCRE(42) through CONCRE(49).

Table 7.1. Namelist Input Variables

Variable Name	Type	Dimensions	Units	Default Value	Description
INITIALIZATION FLAG					
NLTEID	I*4	—	—	0	Non-LTE radiative transfer (RT) flag (if $\neq 0$, use CRE RT model for line transport)
SPATIAL GRID PARAMETERS					
IGEOM	I*4	—	—	3	Coordinate index (1 – planar, 2 – cylindrical, 3 – spherical)
NZONES	I*4	—	—	0	Number of spatial zones in RT grid (Maximum number = MXZONS)
DRADMN	R*8	—	cm	0.	Width of zone nearest the outer plasma boundary

Variable Name	Type	Dimensions	Units	Default Value	Description
ATOMIC MODEL PARAMETERS					
NGASES	I*4	—	—	1	Number of gas species (maximum number = MXGASS)
ATOMNM	R*8	NGASES	—	0.	Atomic number
ATOMWT	R*8	NGASES	amu	0.	Atomic weight
FRACSP	R*8	NZONES, NGASES	—	1 for igas=1 0 for igas>1	Fractional concentration of gases in each zone Example for homogeneous binary plasma with 20 zones: FRACSP(1,1) = 20*0.5 FRACSP(1,2) = 20*0.5 Example for layered plasma: FRACSP(1,1) = 10*1., 10*0. FRACSP(1,2) = 10*0., 10*1.
ISELCT	I*4	MXLVLI, MXGASS	—	0	Array to select atomic levels from atomic data files 1 ⇒ on (or select); 0 ⇒ off (default)
RADIATIVE TRANSFER PARAMETERS					
ILINEP	I*4	—	—	1	Line profile type (1 ⇒ Doppler; 2 ⇒ Lorentz; 3 ⇒ Voigt)
ISWCRE (7)	I*4	100	—	0	Compute photoexcitation if equal to 0
ISWCRE (8)	I*4	100	—	0	Compute photoionization if equal to 0

Variable Name	Type	Dimensions	Units	Default Value	Description
OTHER PARAMETERS					
CONCRE	R*8	100	—	See Table 7.2	Array of constants (see Table 7.2)
ISWCRE	I*4	100	—	0	Array of integer switches (see Table 7.3)
IEDCRE	I*4	100	—	0	Array of edit (debugging) flags (see Table 7.4)
IBENCH	I*4	20	—	0	Array used for benchmark test calculations IBENCH(3) = 1: 2-level atom with $\kappa \propto r^{-2}$ 2: 2-level atom with $\kappa \propto r^{-2}$ and $B_\nu \propto r^{-2}$ (spherical case; see [34])
IPLOT	I*4	30	—	0	Array of plot switches (currently not used)
CONVERGENCE PARAMETERS					
ERRMXF	R*8	—	—	1.e-3	Maximum error allowed in fractional populations during convergence procedure
IMAXSE	I*4	—	—	40	Maximum number of iterations during convergence procedure
CRSWCH	R*8	20	—	1.0	Collisional-radiative switching parameters (used in subroutine STATEQ; see [35]) (generally not needed for laboratory plasmas)
NGCYCL	I*4	—	—	4	Apply Ng acceleration every NGCYCL'th cycle
NGORDR	I*4	—	—	2	Order of Ng acceleration
NGBEGN	I*4	—	—	0	Iteration cycle at which to begin Ng acceleration

Table 7.2. Real Constants - CONCRE

Array Element	Default Value	Description
6	1.e-30	Minimum value of fractional level population
12	0.1	Scaling parameter for statistical equilibrium matrix elements
19	1.e-5	Minimum fractional population used to test convergence
20	1.0	Multiplier for natural line width
21	1.0	Multiplier for Doppler line width
22	1.0	Multiplier for Stark line width
23	1.0	Multiplier for Voigt profile broadening parameter (see also ISWCRE (23))
24	1.0	Multiplier for ion dynamic broadening (hydrogenic Lyman series)
26	1.0	Multiplier for bound-bound opacity
27	1.0	Multiplier for bound-free opacity
28	1.0	Multiplier for free-free opacity
42	1.0	Multiplier for collisional deexcitation rate
43	1.0	Multiplier for spontaneous emission rate
45	1.0	Multiplier for collisional recombination rate
46	1.0	Multiplier for radiative recombination rate
47	1.0	Multiplier for dielectronic recombination rate
57	0.3	Minimum value of $\Delta E/T$ for ionization windowing
58	30.	Maximum value of $\Delta E/T$ for ionization windowing

Table 7.3. Control Switches - ISWCRE

Array Element	Value*	Description
6	0	Start with populations from previous hydro time step
	1*	Start with LTE populations
	2	Start with coronal populations
	3	Return LTE populations
	4	Return coronal populations
7	0*	Include photoexcitation effects in calculation of atomic level populations
8	0*	Include photoionization effects in calculation of atomic level populations
20	0*	Non-LTE equation of state: $E = E_{ion} + E_e + E_{iz}$
	1	$E = E_{ion} + E_e + E_{iz} + E_{degen}$
	2	$E = E_{ion} + E_e + E_{iz} + E_{DH}$
	3	$E = E_{ion} + E_e + E_{iz} + E_{degen} + E_{DH}$
23	0*	Compute Voigt parameter
	1	Set Voigt parameter = CONCRE (23)
	2	Estimate T and a_{voigt} from rate coefficients
30	0	Compute $\bar{g}$ in Stark width calculation
	1*	Set $\bar{g} = 0.2$ in Stark width calculation
34	0*	Use LAPACK matrix scaling
	1	Use LAPACK + NLTERT matrix scaling
38	0*	No equation of state calculation
	1	Compute internal energy and pressure (Not currently an option)
39	0*	No multigroup opacity calculation
	1	Compute multigroup opacities (Not currently an option)
99	0*	Dump output and stop when ill-conditioned matrix is encountered
*An asterisk (*) indicates default value.		

Table 7.4. Debugging Switches - IEDCRE

Array Element	Subroutine Writing Debug Output
7	ABSEMS
18	CCSLAB
18	CLSLAB
12,55	GETCF1
12,55	GETCF2
16	GETPOP
78	GPOPAC
48	IIXSEC
44	INITC2
28,29	INNLTE
32	IZWNDO
61	LINEPR
66,80	LINWID
62	LODCB1
62	LODCB2
11,27	LOPACS
1,14,54	MATRX0
77	MESHMG
78	MGOPAC
34	NGACCL
63	NLPOPS
41	RATCOF
47,81	READA2
6,15	STATEQ
92	VOIGT
81	WSTARK

8. Subroutines

Table 8.1 lists the name of each subroutine of the CRE/radiative transfer model along with a brief description of its primary function. A flow diagram showing the relation of the higher level subroutines is shown in Fig. 8.1. With the exception of using NAMELIST input, all subroutines are written in FORTRAN 77.

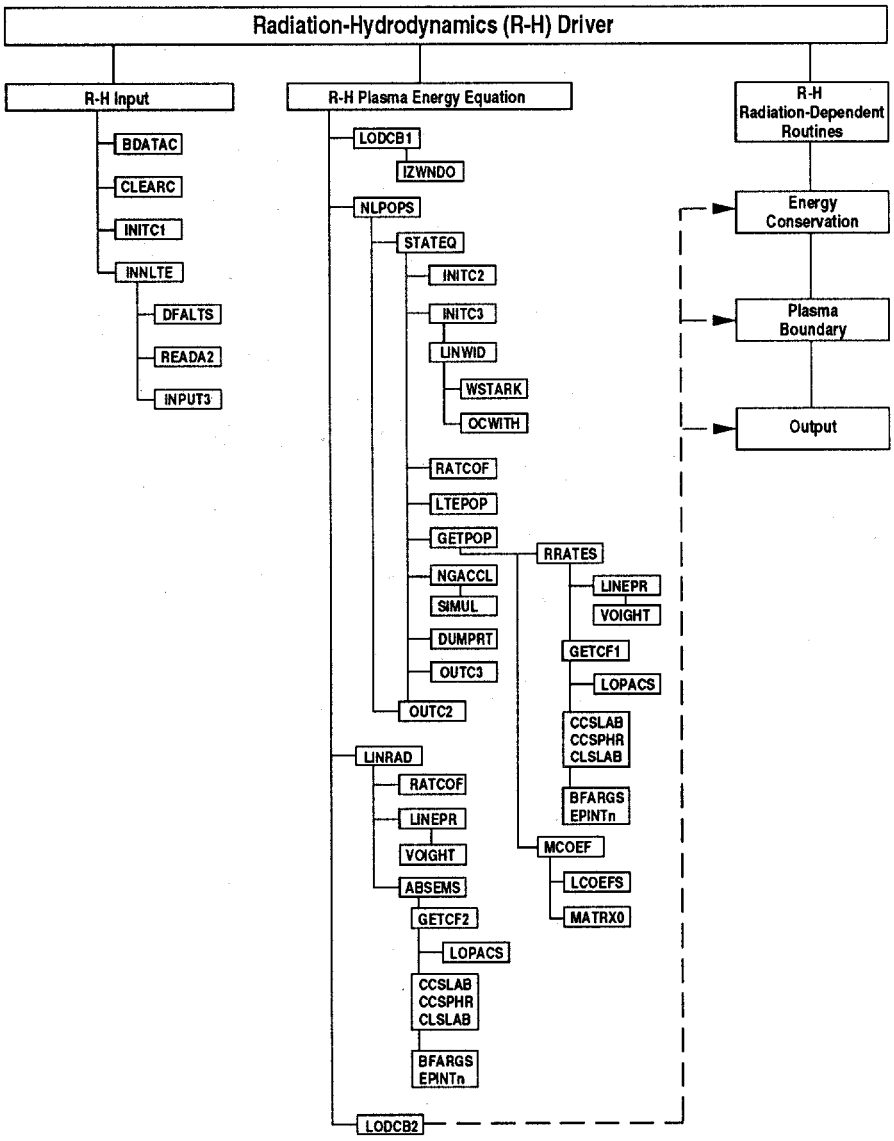

Figure 8.1. Flow diagram for selected subroutines of CRE/radiative transfer model.

Table 8.1. CRE Radiative Transfer Subroutines

Subroutine Name	Called By	Calls To	Description
BDATAC	—	—	Block data routine for initializing constants.
ABSEMS	LINRAD	GETCF2	Computes line power densities and fluxes.
BFARGS	CCSLAB, CCSPHR, CLSLAB	—	Sets up bound-free escape probability parameters.
CLSLAB	GETCF1, GETCF2	EPINT1	Computes escape probability coupling coefficients for Doppler profiles in planar geometry.
CLSLAB	GETCF1, GETCF2	EPINT9, BFARGS	Computes escape probability coupling coefficients for bound-free transitions in planar geometry.
CCSPHR	GETCF1, GETCF2	EPINT2, EPINT3, BFARGS	Computes escape probability coupling coefficients for bound-bound and bound-free transitions in planar geometry.
DFALTS	INNLTE	—	Initialize variables and set default values.
CLEARC	Hydro initialization subroutine	—	Initializes some variables to zero.
DUMPRT	MATRX0, STATEQ	—	Writes CRE radiative transfer parameters to output files.
EPINT1	CLSLAB, CCSPHR	—	Computes escape probability integral for a Doppler profile.
EPINT2	CLSLAB, CCSPHR	—	Computes escape probability integral for a Lorentz profile.
EPINT3	CLSLAB, CCSPHR	—	Compute escape probability integral for a Voigt profile.
EPINT9	CLSLAB, CCSPHR	—	Compute escape probability integral for bound-free transitions.
GETCF1	RRATES	CCSLAB, CCSPHR, CLSLAB, LOPACS	Compute zone-to-zone coupling coefficients for all transitions.

Table 8.1 (Continued)

Subroutine Name	Called By	Calls To	Description
GETCF2	ABSEMS	CCSLAB, CCSPHR, CLSLAB, LOPACS	Compute zone-to-zone coupling coefficients for all transitions.
GETPOP	STATEQ	MCOEF1, RRATES	Computes atomic level populations for all gas species.
INITC1	Hydro initialization subroutine	—	Initialize some atomic parameters and print out control switches and constants.
INITC2	STATEQ	—	Initialize radiative transfer parameters.
INITC3	STATEQ	LINWID	Initialize line profile parameters.
INNLTE	Hydro initialization subroutine	INPUT3, READA2, DFALTS	Input controller routine.
INPUT3	INPUT	—	Reads in photoionization data.
IZWNDO	LODCB1	—	Sets range of ionization stages to be considered for each spatial zone.
LCOEFS	MCOEF0	—	Sets up statistical equilibrium matrix coefficients.
LINEPR	LINRAD, RRATES	VOIGT	Computes line profile parameters.
LINWID	INITC3	WSTARK, OCWITH	Sets up line broadening parameters.
LOPACS	GETCF1, GETCF2	—	Computes source functions and opacities for a given line.
LTEPOP	STATEQ	—	Computes LTE populations for each zone.
MATRX0	MCOEF1	LAPACK routines	Inverts statistical equilibrium matrix to get atomic level populations for 1 spatial zone.
MCOEF1	GETPOP	LCOEFS, MATRX0	Sets up and solves statistical equilibrium equations for all zones.
LINRAD	Hydro plasma energy subroutines	RATCOF, LINEPR, ABSEMS	Computes line radiation absorption and emission rates for each spatial zone.

Table 8.1 (Continued)

Subroutine Name	Called By	Calls To	Description
LODCB1	Hydro plasma energy subroutines	IZWNDO	Loads hydro parameters into CRE common blocks.
LODCB2	Hydro plasma energy subroutines	—	Loads CRE results into hydro common blocks.
NGACCL	STATEQ	SIMUL	Ng acceleration algorithm.
NLPOPS	Hydro plasma subroutine	STATEQ, OUTC2	Computes non-LTE atomic level populations.
OCWITH	LINWID	—	Sets up line broadening parameters for H-like ions at high density.
OUTC2	STATEQ, NLPOPS	—	Prints out atomic level populations.
OUTC3	STATEQ	—	Prints out transition rates.
RATCOF	STATEQ, LINRAD	—	Calculates collisional and radiative rate coefficients.
READA2	INNLTE	—	Reads in atomic data.
RRATES	GETPOP	LINEPR, GETCF1	Computes radiation-dependent rate coefficients.
SIMUL	NGACCL	—	Solves a set of linear equations (for small matrices only).
STATEQ	NLPOPS	INITC2, INITC3, RATCOF, LTEPOP, GETPOP, NGACCL, OUTC3, OUTC2, DUMPRT	Determines distribution of atomic populations from self-consistent solution of statistical equilibrium equations and radiation field.
VOIGT	LINEPR,	—	Compute Voigt line profile.
WSTARK	LINWID	AVG	Computes Stark width for a given line.

9. Common Blocks

Listed in Table 9.1 are the common blocks used in the CRE radiative transfer routines. For each common block, the variable name, type, dimensions, and a brief description of each variable is provided. In most cases, the dimensions of variables are specified by quantities defined in parameter statements. These parameters are:

Parameter	Description
MXLVLS	Maximum number of atomic levels
MXTRNS	Maximum number of atomic transitions
MXGASS	Maximum number of gas species
MXIONZ	Maximum number of ionization stages (per gas species)
MXLVLI	Maximum number of levels in atomic data file
MXPHOT	Maximum number of frequency points in spectral calculation
MXZONS	Maximum number of spatial zones
MXDATT	Maximum number of temperatures in rate coefficient tables
MXDATD	Maximum number of electron densities in rate coefficient tables
MXSSHL	Maximum number of atomic subshells
MXGRPS	Maximum number of groups for multigroup opacity calculation.

Table 9.1. Common Blocks

COMMON/ATDATA/

Variable	Type	Dimensions	Units	Description
TEMIN	R*8	MXGASS	eV	Minimum electron temperature for rate coefficient grid
DLOGTE	R*8	MXGASS	–	Logarithmic increment (base 10) of electron temperature for rate coefficient grid
DEMIN	R*8	MXGASS	cm^{-3}	Minimum electron density for rate coefficient grid
DLOGDE	R*8	MXGASS	—	Logarithmic increment (base 10) of electron density for rate coefficient grid
CLDEXA	R*4	MXDATT, MXTRNS	$cm^3\ s^{-1}$	Collision excitation rate coefficient due to thermalized electrons
SPNEMA	R*8	MXTRNS	s^{-1}	Spontaneous emission rate
CLRECA	R*4	MXDATT, MXTRNS	$cm^6\ s^{-1}$	Collisional recombination rate coefficient due to thermalized electrons
RDRECA	R*4	MXDATT, MXTRNS	$cm^3\ s^{-1}$	Radiative recombination rate coefficient
DIELRA	R*4	MXDATT, MXDATD, MXTRNS	$cm^3\ s^{-1}$	Dielectronic recombination rate coefficient
NDATTE	I*4	MXGASS	—	Number of points in temperature grid of atomic data file
NDATDE	I*4	MXGASS	—	Number of points in electron density grid of atomic data file

Values for the above variables are read in from ATBASE files and stored.

COMMON/ATOMIC/

Variable	Type	Dimensions	Units	Description
ATOMWT	R*8	MXGASS	amu	Atomic weight
FRACSP	R*8	MXZONS, MXGASS	—	Fractional abundance (by number density) of each gas species
STATWT	R*8	MXLVLS	—	Statistical weight
ENERGY	R*8	MXLVLS	eV	Atomic level energy measured relative to fully ionized
EREFER	R*8	MXGASS	eV	Reference energy for equation of state calculation
ENBIND	R*8	MXLVLS, MXSHEL	a.u. (=27.2 eV)	Electron binding energy used for Stark width calculation
STRKR2	R*8	MXLVLS, MXSHEL	a.u. ($=a_o$)	Electron mean squared orbital radius for Stark width calculation
STRKDE	R*8	MXLVLS	a.u.	Energy to nearest level for Stark width calculation
STARKF	R*8	MXLVLS	—	Gaunt factor parameter for Stark width calculation
STKRI	R*8	MXLVLS	a.u.	Orbital radius of level of interest for Stark width calculation
STKRIP	R*8	MXLVLS	a.u.	Orbital radius of nearest level for Stark width calculation
NLEVLS	I*4	—	—	Total number of atomic levels
IONSTG	I*4	MXLVLS	—	Ionization stage (1 ⇒ neutral)
IGROUN	I*4	MXGASS, MXIONZ	—	Level index of ground sate for each ion
NGASES	I*4	—	—	Number of gas species

COMMON/ATOMIC/ (Continued)

Variable	Type	Dimensions	Units	Description
LKMIN	I*4	MXGASS	—	Index of first (lowest) energy level for each gas species
LKMAX	I*4	MXGASS	—	Index of last (highest) energy level for each gas species
NLEVLK	I*4	MXGASS	—	Number of energy levels for each gas species
LKJMIN	I*4	MXGASS, MXIONZ	—	Index for first (lowest) energy level for each ion
LKJMAX	I*4	MXGASS, MXIONZ	—	Index of last (highest) energy level for each ion
IZGAS	I*4	MXGASS,	—	Atomic number of each gas
KGAS	I*4	MXLVLS	—	Gas species index
LMINZN	I*4	MXZONS, MXGASS	—	Index of lowest energy level for each gas in each zone
LMAXZN	I*4	MXZONS, MXGASS	—	Index of highest energy level for each gas in each zone
NLEVZN	I*4	MXZONS, MXGASS	—	Index of energy levels for each gas in each zone

COMMON/ATRANS/

Variable	Type	Dimensions	Units	Description
ETRANS	R*8	MXTRNS	eV	Transition energy
OSCSTR	R*8	MXTRNS	—	Oscillator strength
PROFLC	R*8	MXZONS, MXTRNS	Hz^{-1}	Value of line profile at line center ($\int \phi_\nu d\nu = 1$)
AVOIGT	R*8	MXZONS, MXTRNS	—	Voigt profile damping parameter
TAUTOT	R*8	MXTRNS	—	Total optical depth for each transition
WIDNAT	R*8	MXTRNS	eV	Natural line width
WIDDOP	R*8	MXTRNS	$eV^{3/2}$	Doppler line width
WIDSTK	R*8	MXZONS, MXTRNS	$eV^{3/2}$ cm^3	Stark line width
WIDION	R*8	MXZONS, MXTRNS	eV	Stark ion dynamic broadening
ILINEP	I*4	—	—	Line profile type (1 ⇒ Doppler; 2 ⇒ Lorentz; 3 ⇒ Voigt)
ITTYPE	I*4	MXTRNS	—	Transition type (1 ⇒ bound-bound; 6-10 ⇒ bound-free)
LUPPER	I*4	MXTRNS	—	Upper level index of transition
LLOWER	I*4	MXTRNS	—	Lower level index of transition
NTRANS	I*4	—	—	Total number of transitions
MINTRN	I*4	MXGASS	—	Minimum transition index of gas
MAXTRN	I*4	MXGASS	—	Maximum transition index of gas
LTRANS	I*2	MXLVLS, MXLVLS	—	Transition index for (upper, lower) levels

COMMON/CONSTS/

Variable	Type	Dimensions	Units	Description
HPLANK	R*8	—	eV s	Planck's constant
BOLTZK	R*8	—	—	Boltzmann's constant
CLIGHT	R*8	—	cm s^{-1}	Speed of light
AMUMAS	R*8	—	g	Atomic mass unit
RYDBRG	R*8	—	eV	Rydberg (= 13.6 eV)
RGASCN	R*8	—	erg mol^{-1} K^{-1}	Gas constant ($= 8.3146 \times 10^7$)
ZERO	R*8	—	—	Zero
ONE	R*8	—	—	One
TWO	R*8	—	—	Two
HALF	R*8	—	—	One-half
THIRD	R*8	—	—	One-third
SIXTH	R*8	—	—	One-sixth
PI	R*8	—	—	π
FOURPI	R*8	—	—	4π
SQRTPI	R*8	—	—	$\pi^{1/2}$
SPIINV	R*8	—	—	$\pi^{-1/2}$
ERG2EV	R**	—	eV erg^{-1}	Energy conversion factor ($= 6.242 \times 10^{11}$)
EV2K	R*8	—	K eV^{-1}	Temperature conversion factor ($= 11,606$)

COMMON/CONTRL/

Variable	Type	Dimensions	Units	Description
CONCRE	R*8	100	—	Array of constants (see Table 6.2)
XMUBAR	R*8	—	—	Mean cosine angle for escape probability model
XMULOS	R*8	—	—	Cosine angle of line-of-sight for emergent flux calculation
ERRMXF	R*8	—	—	Maximum fractional error in atomic level populations
CRSWCH	R*8	20	—	Collisional-radiative switching parameter
NGCYCL	I*4	—	—	Apply Ng acceleration every NGCYCL'th cycle
NGORDR	I*4	—	—	Order of Ng acceleration
NGBEGN	I*4	—	—	Iteration cycle to begin Ng acceleration
ISWCRE	I*4	100	—	Array of switches (see Table 6.3)
IPLOT	I*4	30	—	Array of switches (see Section 6)
IEDCRE	I*4	100	—	Array of debug switches (see Table 6.4)
IMAXSE	I*4	—	—	Maximum number of iterations for statistical equilibrium cycle
IBENCH	I*4	20	—	Switch for benchmarking calculations

COMMON/CREOUT/

ABSRAT	R*8	MXZONS	erg cm^{-3} s^{-1}	Line radiation absorption rate
EMSRAT	R*8	MXZONS	erg cm^{-3} s^{-1}	Line radiation emission rate
FLUXBD	R*8	MXZONS	erg cm^{-2} s^{-1}	Line radiation flux escaping plasma boundary

COMMON/FILUNS/

LUN	I*4	100	—	Logical unit numbers of input and output files
FNAMES	C*16	100	—	File names of input and output files

COMMON/GRID/

Variable	Type	Dimensions	Units*	Description
RADCRE	R*8	MXZONS+1	cm	Spatial zone boundaries
DRAD	R*8	MXZONS	cm	Zone width
RBAR	R*8	MXZONS	cm	Position of zone midpoint
DRAY	R*8	MXZONS, MXZONS	—	Parameters used in escape probability model
DDRAY	R*8	MXZONS, MXZONS	—	Parameters used in escape probability model
DRAYS	R*8	MXZONS, MXZONS	—	Parameters used in escape probability model
DDRAYS	R*8	MXZONS, MXZONS	—	Parameters used in escape probability model
XNEONA	R*8	MXZONS, MXZONS MXGASS	—	Ratio of number of atoms in emitting zone to that in absorbing zone
VOLZON	R*8	MXZONS	cm^{α}	Volume in each spatial zone
VOLTOT	R*8	—	cm^{α}	Total volume of plasma
GEOMA	R*8	3	—	$(1,2\pi,4\pi)$ for IGEOM = (1,2,3)
GEOMV	R*8	3	—	$(1,\pi,4\pi/3)$ for IGEOM = (1,2,3)
DELROZ	R*8	MXZONS, MXIMPS	—	$(\Delta r/\Delta z)$ for spherical radiative transfer calculation

COMMON/GRID/ (Continued)

Variable	Type	Dimensions	Units*	Description
NZONES	I*4	—	—	Number of spatial zones
IGEOM	I*4	—	—	Geometry index*

$$^{*}\alpha = \text{IGEOM} = \begin{cases} 1 & \text{planar} \\ 2 & \text{cylindrical} \\ 3 & \text{spherical} \end{cases}$$

KMINCP	I*4	MXZONS	—	Zone indexing parameters for coupling coefficient calculation

COMMON/PIXSEC/

HVEDGE	R*8	MXTRNS	eV	Energy of photoionization edge ($h\nu_1$)
PIXS0	R*8	MXTRNS	cm^2	Photoionization cross section at threshhold
PIBETA	R*8	MXTRNS	—	"β" in cross section fit*
PISEXP	R*8	MXTRNS	—	"s" in cross section fit*
MNHVPI	I*4	MXTRNS	—	Minimum photon energy index such that $\nu \geq \nu_1$

*Photoionization cross sections are fit to:

$$\alpha(\nu) = \alpha(\nu_1) \left\{ \beta \left(\frac{\nu_1}{\nu} \right)^s + (1-\beta) \left(\frac{\nu_1}{\nu} \right)^{s+1} \right\} , \qquad \nu \geq \nu_1 \, .$$

COMMON/POPULS/

Variable	Type	Dimensions	Units	Description
POPUL	R*4	MXLVLS, MXZONS	—	Fractional atomic level populations

COMMON/RADCFS/

CCCFS	R*8	MXZONS, MXTRNS	—	"Residual" of Λ-operator
CCFS1	R*8	MXZONS, MXTRNS	—	"Diagonal" of Λ-operator

COMMON/RADTRN/

CCOEFS	R*8	MXZONS, MXZONS	—	Zone-to-zone coupling coefficients
TAU	R*8	MXZONS+1	—	Optical depth integrated from plasma surface
DTAU	R*8	MXZONS	—	Optical depth for each zone

COMMON/RATCFS/

Variable	Type	Dimensions	Units	Description
COLEXC	R*8	MXZONS, MXTRNS	$cm^3\ s^{-1}$	Collisional excitation rate coefficient
COLDEX	R*8	MXZONS, MXTRNS	$cm^3\ s^{-1}$	Collisional deexcitation rate coefficient
COLLIZ	R*8	MXZONS, MXTRNS	$cm^3\ s^{-1}$	Collisional ionization rate coefficient
COLREC	R*8	MXZONS, MXTRNS	$cm^6\ s^{-1}$	Collisional recombination rate coefficient
RADREC	R*8	MXZONS, MXTRNS	$cm^3\ s^{-1}$	Radiative recombination rate coefficient
DIELRC	R*8	MXZONS, MXTRNS	$cm^3\ s^{-1}$	Dielectronic recombination rate coefficient
SPONEM	R*8	MXTRNS	s^{-1}	Spontaneous emission rate

COMMON/SPECTR/

HVMIN	R*8	—	eV	Minimum photon energy of spectral calculation
HVMAX	R*8	—	eV	Maximum photon energy of spectral calculation
NFRQFF	I*4	—	—	Number of continuum photon energy points in spectral grid
NFRQBB	I*4	—	—	Number of photon energy points per bound-bound transition

COMMON/STRING/

Variable	Type	Dimensions	Units	Description
CONFIG	C*130	MXLVLS	—	Atomic configuration
TRMSYM	C*10	MXLVLS	—	Atomic term symbol

COMMON/THERMO/

TEMPEL	R*8	MXZONS	eV	Electron temperature
TMPION	R*8	MXZONS	eV	Ion temperature
DENSNN	R*8	MXZONS	cm^{-3}	Ion number density
DENSNE	R*8	MXZONS	cm^{-3}	Electron density

Acknowledgments

This work has been supported in part by Kernforschungszentrum Karlsruhe through Fusion Power Associates, and by U.S. Department of Energy Contract No. DE-AS03-88DP10754 through the University of Wisconsin.

References

[1] J. Davis, K.G. Whitney, and J.P. Apruzese, *J. Quant. Spectrosc. Radiat. Transfer* **20**, 353 (1978).

[2] B.F. Rozsnyai, *J. Quant. Spectrosc. Radiat. Transfer* **27**, 211 (1982).

[3] D. Duston, R.W. Clark, J. Davis, and J.P. Apruzese, *Phys. Rev.* **A 27**, 1441 (1983).

[4] S. Maxon and T. Wainwright, *Phys. Fluids* **27**, 2535 (1984).

[5] J.E. Rogerson, R.W. Clark, and J. Davis, *Phys. Rev.* **A 31**, 3323 (1985).

[6] D. Duston, R.W. Clark, and J. Davis, *Phys. Rev.* **A 31**, 3220 (1985).

[7] R.W. Clark, J. Davis, and F.L. Cochran, *Phys. Fluids* **29**, 1971 (1986).

[8] J.J. MacFarlane, P. Wang, and G.A. Moses, *Fusion Tech.* **19**, 703 (1990).

[9] R.R. Peterson, J.J. MacFarlane, and G.A. Moses, "CONRAD – A Combined Hydrodynamics Vaporization/Condensation Computer Code," Univ. of Wisconsin Fusion Technology Institute Report UWFDM-670 (1988).

[10] J.J. MacFarlane and P. Wang, *Phys. Fluids* **B3**, 3494 (1991).

[11] M. Morakami and J. Meyer-ter-Vehn, *Nucl. Fusion* **31**, 1315 (1991).

[12] J.J. MacFarlane and P. Wang, *Lasers Part. Beams* **10**, 349 (1992).

[13] J.J. MacFarlane, P. Wang, and G.A. Moses, Fusion Power Associates Report No. FPA-90-1, January 1990.

[14] J.J. MacFarlane, P. Wang, and D.L. Henderson, Fusion Power Associates Report No. FPA-91-1, January 1991.

[15] J.J. MacFarlane, P. Wang, and D.L. Henderson, Fusion Power Associates Report No. FPA-92-1, January 1992.

[16] J.J. MacFarlane, P. Wang, D.L. Henderson, and O. Yasar, Fusion Power Associates Report No. FPA-93-1, January 1993.

[17] P. Wang, ATBASE Users' Guide, Fusion Power Associates Report No. FPA-93-7, December 1993.

[18] E. Anderson et al., LAPACK Users' Guide (SIAM, Philadelphia, 1992).

[19] K. Werner and D. Husfield, *Astron. Astrophys.* **148**, 417 (1985).

[20] J.J. MacFarlane, *Astron. Astrophys.* **264**, 153 (1992).

[21] K.C. Ng, *J. Chem. Phys.* **61**, 2680 (1974).

[22] L. Auer, in Numerical Radiative Transfer, edited by W. Kalkoten, Cambridge University Press, Cambridge, U.K. (1987), p. 101.

[23] J.P. Apruzese, J. Davis, D. Duston, and K.G. Whitney, *J.Q.S.R.T.* **23**, 479 (1980).

[24] J.P. Apruzese, *J.Q.S.R.T.* **25**, 419 (1981).

[25] J.P. Apruzese, *J.Q.S.R.T.* **34**, 447 (1985).

[26] D. Mihalas, Stellar Atmospheres, Second Edition, Freeman and Company, New York (1978).

[27] P. Wang, Ph.D. Dissertation, Dept. of Nuclear Engineering and Engineering Physics, University of Wisconsin, Madison, WI (1991).

[28] A. Burgess and M.C. Chidichchimo, *Mon. Not. R. Astron. Soc.* **203**, 1269 (1983).

[29] M.J. Seaton, in Atomic and Molecular Processes, edited by D.R. Bates, Academic, New York (1962) p. 374.

[30] I.I. Sobelman, L.A. Vainshtein, and E.A. Yukov, Excitation of Atoms and Broadening of Spectral Lines, Springer-Verlag, New York (1981).

[31] D.E. Post, R.V. Jensen, C.B. Tarter, W.H. Grasberger, and W.A. Lokke, *At. Data Nucl. Data Tables* **20**, 397 (1977).

[32] R.W. Clark and J.P. Apruzese, private communication (1991).

[33] J.J. MacFarlane, NLTERT Users' Guide, Fusion Power Associates Report No. FPA-93-6.

[34] P.B. Kunacz and D.G. Hummer, *Mon. Not. Royal Astr. Soc.* **166**, 19 (1974).

[35] D.G. Hummer and S.A. Voels, *Astron. Astrophys.* **192**, 279 (1988).